Electronic Supplementary Material

Constructing plasmonic electron acceptors on TiO_2 for full-spectrum-driven photocatalytic hydrogen generation

Changhai Lu, [#a,b] Xiaoyan Cai, [# c] Xiaolei Liu, [a] Dehua Tian, [a] Baojun Li, [a] Juan Li, *[a] Zaizhu Lou*[a]

[a]Guangdong Provincial Key Laboratory of Nanophotonic Manipulation, Institute of Nanophotonics, Jinan University, Guangzhou, 511443, China

[b]Key Laboratory of Jiangxi Province for Persistent Pollutants Control and Resources Recycle, Nanchang Hangkong University, Nanchang, 330063, China

[c]School of Materials Science and Physics, China University of Mining and Technology, Xuzhou 221116, China

Corresponding author: lijuan@jnu.edu.cn, zzlou@jnu.edu.cn

Experimental Section

Synthesis of TiO_2 nanosheets (TO-NSs). Anatase TO-NSs were synthesized by a reported solvothermal method. In a typical procedure, 20 mL $Ti(OC_4H_9)_4$ and 3.2 mL hydrofluoric acid solution (40%) were mixed and transferred to a 50 mL Teflon-lined stainless steel autoclave, heated and maintained at 200 °C for 24 h. After naturally cooling down to room temperature, the blank powder was separated by centrifugation, washed with ethanol and Milli-Q water for three times and dried for overnight.

Synthesis of TiO_2 nanodots (TO-NDs). 134 μL $TiCl_4$ was slowly added into 30 mL ethanol, and then the solution was heated at 180 ℃ for 24 h. After naturally cooling down to room temperature, the dark blue powder was separated by centrifugation, washed with ethanol and Milli-Q water for three times and dried for overnight. The obtained sample was labelled as TO-NDs.

Synthesis of W-doped TiO_2 nanodots (WTO-NDs). 134 μL $TiCl_4$ was slowly added into 30 mL ethanol. Subsequently, 4.76 mg WCl_6 was added into above solution with constant stirring for 10 min, then heated at 180 ℃ for 24 h. After naturally cooling down, the powder was separated by centrifugation, washed and dried for overnight. The W-doped TiO_2 nanodots samples were labelled as WTO-NDs-x (x=0.5, 1, 1.5, 2), where x was the molar percentage of the doped W element.

Synthesis of W-doped TiO_2 nanodots/TiO_2 nanosheets heterostructures (WTO-NDs/TO-NSs). 6.85 μL $TiCl_4$ was slowly added into 10 mL ethanol and then added with 243 μg WCl_6 was by constant stirring for 10 min. 50 mg TO-NSs was dispersed in 15 mL ethanol and then added with the above precursor solution drop by drop. After

stirring for 15 min, the mixture was heated at 180 ℃ for 24 h. The powder was separated by centrifugation, washed and dried for overnight. The obtained sample was labelled as WTO-NDs-1/TO-NSs.

Photocatalytic hydrogen generation test. In a typical photocatalytic reaction, 5 mg WTO-NDs-1/TO-NSs (2wt% Pt was loaded as cocatalyst) were dispersed into mixed solution of 10 mL Milli-Q water and 1 mL triethanolamine, and then was sealed in a glass tube and degassed with pure N_2 for 20 min. Then, the tube was irradiated under UV-visible-NIR light (200 mW cm^{-2}) with magnetic stirring at room temperature. The gaseous products were analysed by gas chromatography (GC-2014A, Shimadzu) equipped with one TCD and two flame ionization detectors (FID). Photocatalytic reaction was also carried out under different light irradiation which is supplied by different-wavelength cutoff filters (< 400nm, 400-780 nm, > 400 nm, > 800 nm).

DFT simulations. All computational simulations were conducted utilizing the DS-PAW simulation software based on density functional theory (DFT) [1]. The interaction between valence electrons and ionic cores was delineated employing projector-augmented waves (PAW) pseudopotentials. During the structural relaxation process, the Perdew-Burke-Ernzerhof (PBE) pseudopotential approximation within the generalized gradient approximation (GGA) was implemented. In the case of TiO_2, all computations were carried out using a 2×2×2 supercell containing 64 oxygen atoms and 32 titanium atoms. For calculations involving W-doped TiO_2, a single tungsten (W) atom replaced a titanium (Ti) atom within the aforementioned supercell. The computational parameters included a cutoff energy (Ecut) of 480 eV, a total energy

convergence threshold of 1×10^{-4} eV, and a residual stress threshold of 0.05 eV/Å. Additionally, a 3×3×1 Monkhorst-Pack k-point grid was employed.

Characterizations. X-ray diffraction (XRD) patterns of sample were carried out by a Rigaku Rint-2500 diffractometer with Cu K_α radiation at a scanning rate of $0.1°\ s^{-1}$. The morphologies were measured by transmission electron microscope (2100, JEOL, operated at 100 kV) and high-resolution TEM (JEM-3000F, operated at 300 kV). X-ray photoelectron spectroscopy (XPS) measurements were performed at a Thermo Fisher Scientific K-ALPHA+ spectrometer with the binding energy referenced to the C 1s peak at 284.6 eV. UV-Vis-NIR diffuse reflectance spectra (UV-Vis-NIR DRS) were recorded on a spectrophotometer (JASO V-570). The electrochemical and photoelectrochemical measurements were measured by a CHI 660D workstation in a three-electrode cell. The time-resolved PL spectra were recorded by using an objective scanning confocal microscope system (PicoQuant, MicroTime 200) coupled with an Olympus IX71 inverted fluorescence microscope. The samples were excited through an oil-immersion objective lens (Olympus, UplanSApochromat, 100×, 1.4 NA) and a circular-polarized 375 nm Plus wave laser controlled by a PDL-800B driver (PicoQuant).

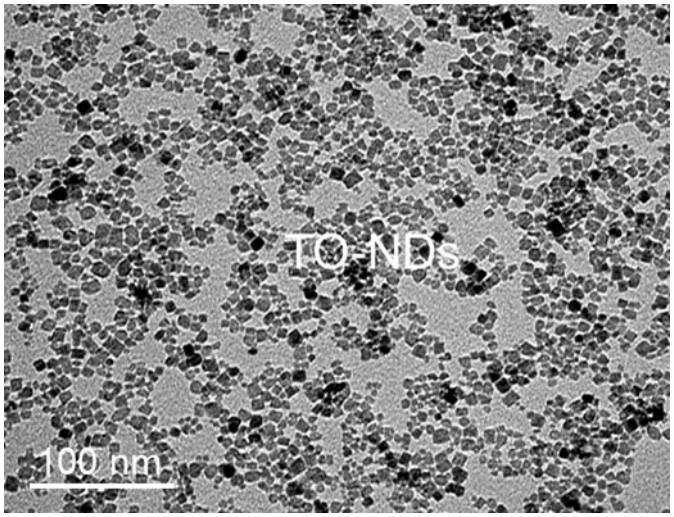

Figure S1. TEM image of TO-NDs

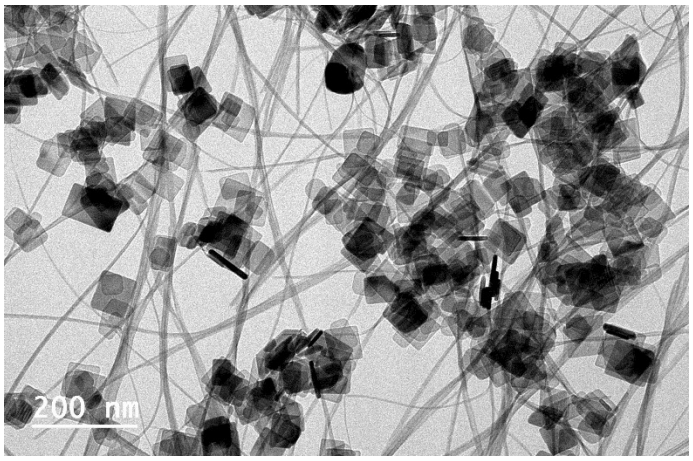

Figure S2. The TEM image of the WO_{3-x}/TO-NSs photocatalyst

Table S1 ICP-OES of WTO-NDs/TO-NSs

Samples	Quality(m_0)（g）	Volume(V_0)（mL）	Test element	element concentration(C_o)（mg/L）	Dilution ratio(f)	C_1（mg/L）	C_x（mg/kg）	element content(W)
WTO-NDs-0.5/TO-NSs	0.0334	10	Ti	17.1289	100	17128.9000	512841.32	51.2841%
WTO-NDs-1.0/TO-NSs	0.0284	10	Ti	15.2332	100	15233.2000	536380.28	53.6380%
WTO-NDs-1.5/TO-NSs	0.0308	10	Ti	16.3230	100	1632.3000	529967.53	52.9968%
WTO-NDs-2.0/TO-NSs	0.0358	10	Ti	19.4361	100	1943.6100	542907.82	54.2908%
WTO-NDs-0.5/TO-NSs	0.0334	10	W	2.7632	1	2.7632	827.31	0.0827%
WTO-NDs-1.0/TO-NSs	0.0284	10	W	5.4289	1	5.4289	1911.58	0.1912%
WTO-NDs-1.5/TO-NSs	0.0308	10	W	10.6820	1	10.6820	3468.18	0.3468%
WTO-NDs-2.5/TO-NSs	0.0358	10	W	15.5633	1	15.5633	4347.29	0.4347%

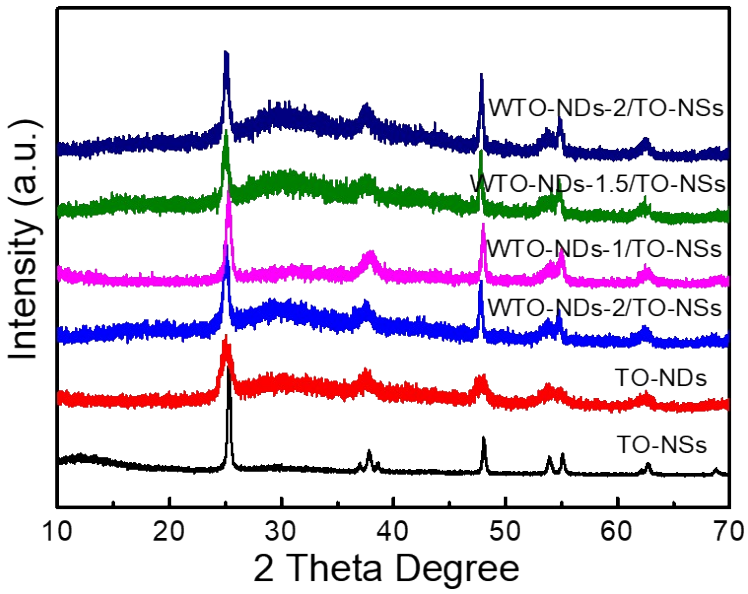

Figure S3. XRD patterns of WTO-NDs/TO-NSs heterostructures

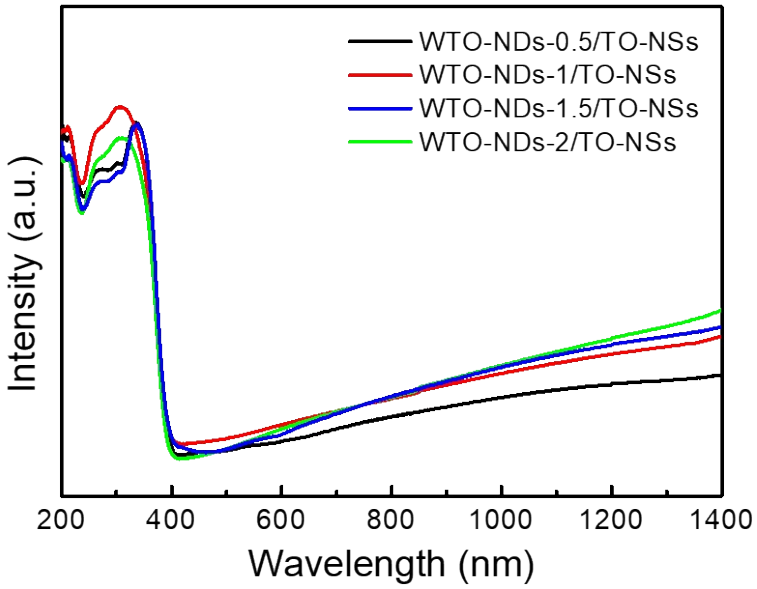

Figure S4. DRS spectral of WTO-NDs/TO-NSs heterostructures

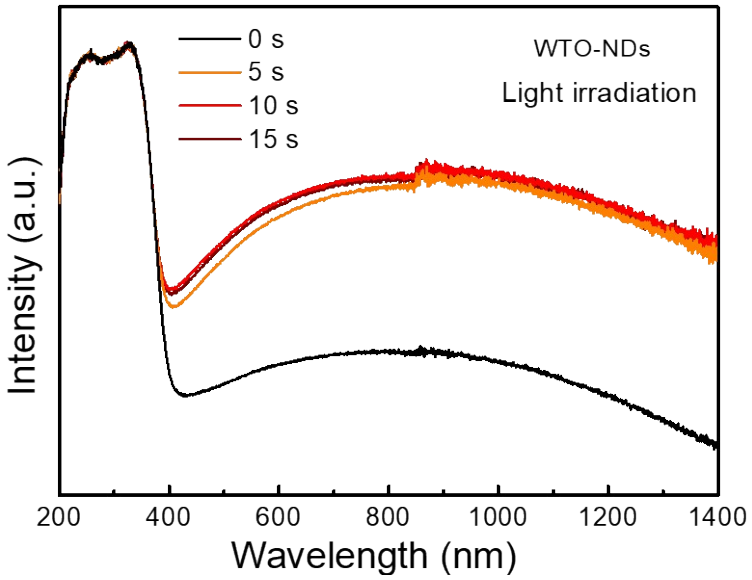

Figure S5. UV-visible NIR DRS variation of WTO-NDs

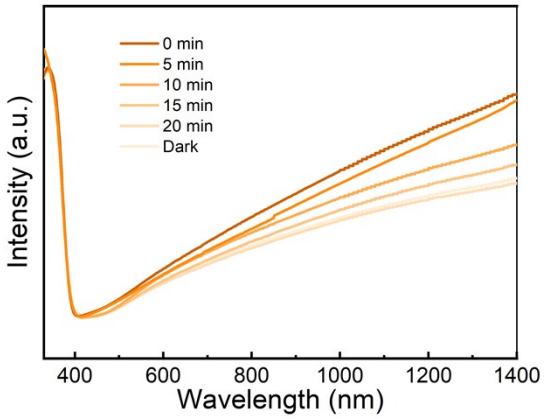

Figure S6. UV-vis-NIR DRS changes of WTO-NDs-1/TO-NSs heterostructure after stopping light irradiation

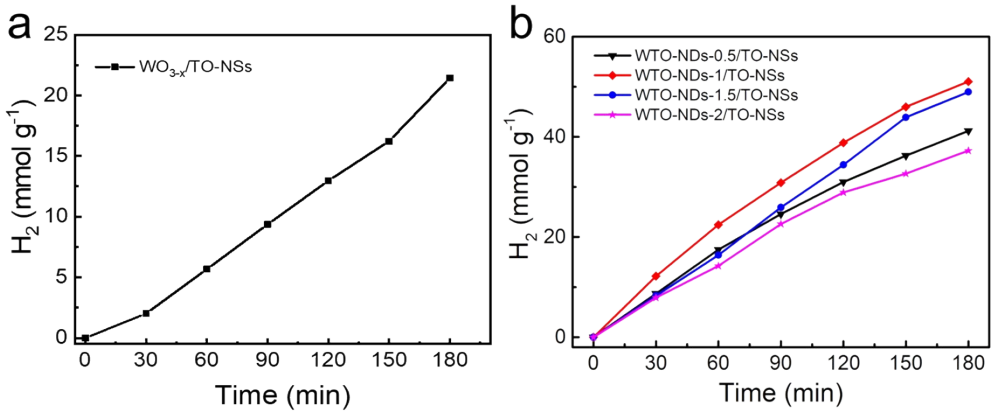

Figure S7. Hydrogen generation over WO_{3-x}/TO-NSs photocatalyst (a) and various WTO-NDs/TO-NSs heterostructures (b)

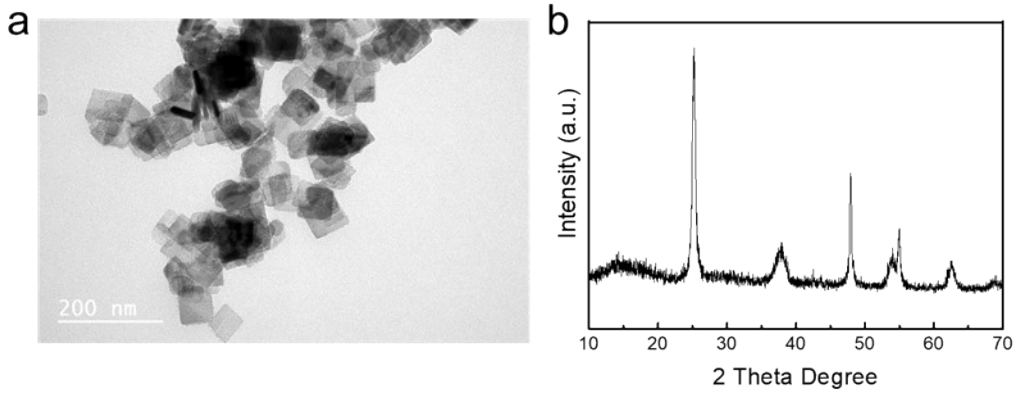

Figure S8. The TEM image and XRD patterns of WTO-NDs/TO-NSs heterostructures after photocatalysis

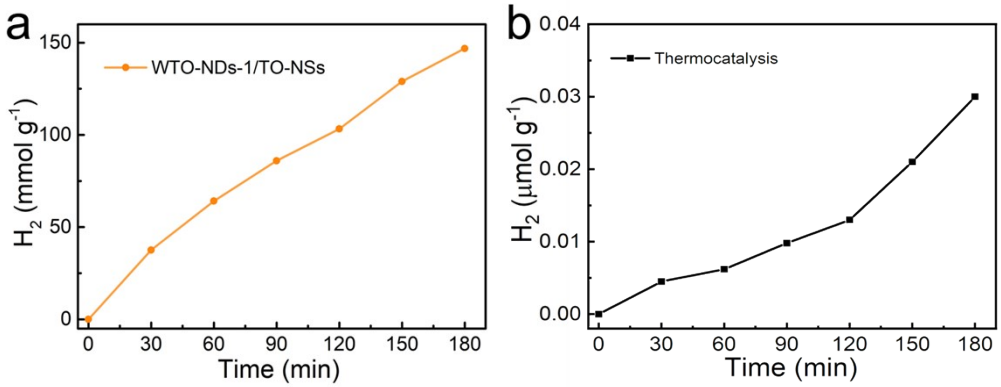

Figure S9. The photothermocatalytic (a) and thermocatalytic (b) hydrogen generation over WTO-NDs-1/TO-NSs heterostructure

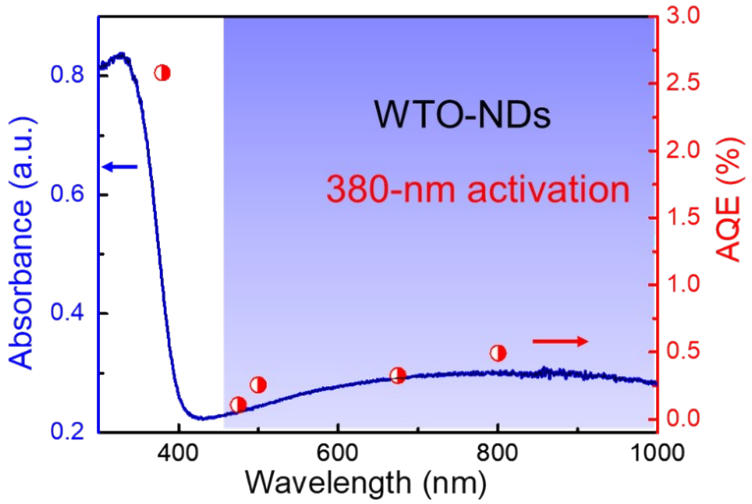

Figure S10. DRS and apparent quantum efficiency (AQE) of WTO-NDs with 380-nm activation during photocatalytic hydrogen generation.

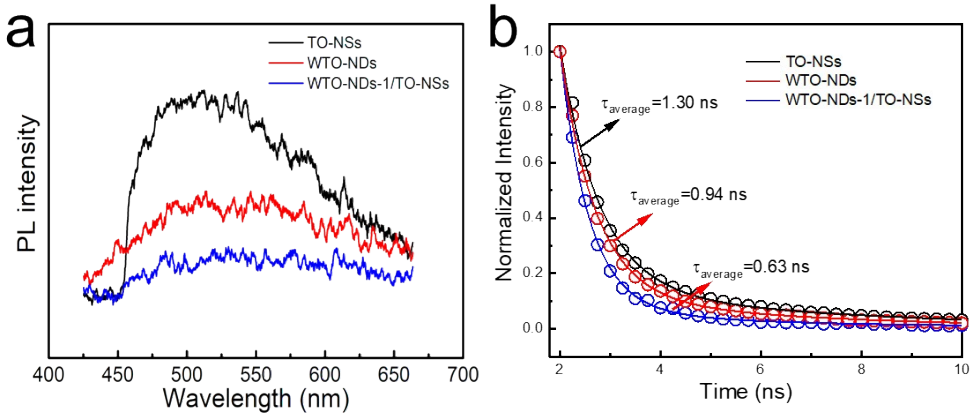

Figure S11. The steady-state and time-resolved PL spectra of TO-NSs, WTO-NDs and WTO-NDs-1/TO-NSs

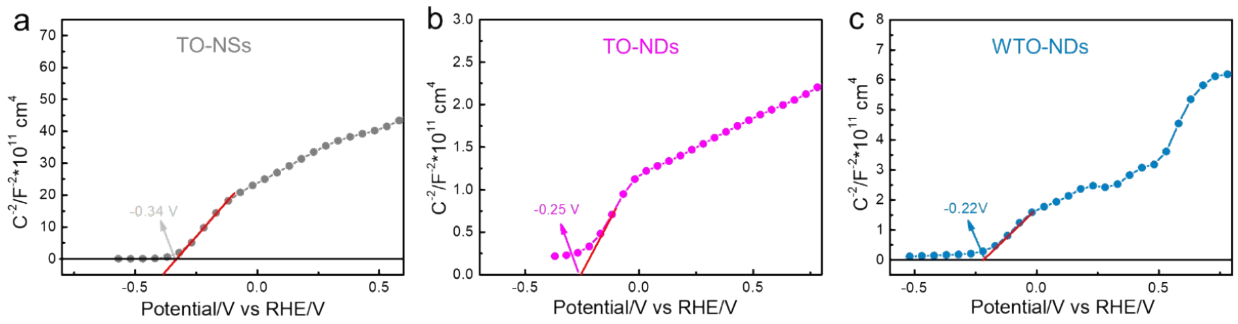

Figure S12. Mott-Schottky plots of TO-NSs, TO-NDs and WTO-NDs measured in a NaOH (1 M; pH 13.6) electrolyte at frequencies 1000 Hz.

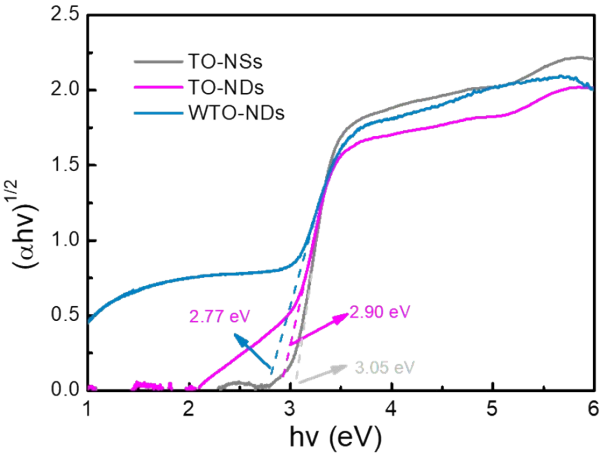

Figure S13. The transformed Kubelka-Munk function vs the energy of light for TO-NSs, TO-NDs and WTO-NDs.

Photocatalysts	Light source	Solution	Rate of H_2 evolution ($\mu mol\ g^{-1}\ h^{-1}$)
$Au_{CSA\text{-}silica}$@TiO_2 NSs	300 W Xe lamp ($\lambda > 495$ nm)	H_2O/ 10 vol% methanol solution	646.0[2]
AuNPs/TiO_2 nanorod	300 W Xe lamp	25 mL ethanol solution	7100[3]
CuO_x@C-Anchored TiO_2	500 W Xe lamp	H_2O/ 10 vol% methanol solution	383[4]
AuNP/TiO_2	300 W Xe lamp	H_2O/ 10 vol% methanol solution	16577[5]
Au/TiO_2/MoS_2	350 W Xe lamp	H_2O/ (10 vol%) Glycerite solution	708.05[6]
CdS/Bi/TiO_2	500 W Xe lamp ($\lambda > 400$ nm)	0.25 M Na_2S + 0.35 M Na_2SO_3	673.81[7]

		solution	
WTO-NDs-1/TO-NSs	300 W Xe lamp	H_2O/ (10 vol%) triethanolamine solution	17010[This work]

Table S2. Photocatalytic hydrogen generation performance of WTO-NDs/TO-NSs heterostructures compare to other catalysts

References

1 P. E. Blochl, *Matter.*, 1994, **50**, 17953-17979.

2 Y. Kim, D. H. Wi, J. W. Hong, S. W. Han, *ACS Nano* 2023, **18**, 18641-18651.

3 X. Zhang, L. Luo, R. P. Yun, M. Pu, B. Zhang, X. Xiang, *ACS Sustainable Chem. Eng.*, 2019, **16**, 13856-13864.

4 P. Liu, A. Dörfler, A. A. Tabrizi, L. Skokan, D. Rawach, P. Wang, Z. Peng, J. M. Zhang, A. P. Ruediger, J. P. Claverie, *ACS Appl. Mater. Interfaces*, 2023, **15**, 23, 27832-27844.

5 J. Zhang, D. Wang, R. Chen, X. Zhu, D. D. Ye, Y. Yang, Q. Liao, *Energ. Convers. Manage.*, 2023, **277**, 116626.

6 Q. Wang, S. Zhu, S. Zhao, C. Li, R. Wang, D. Cao, G. Liu, *Fuel,* 2022*,* **322**, 124163.

7 X. Du, Y. Li, H. Yin, Q. Xing, *Acta Phys. -Chim. Sin*., 2018, **34**, 414-423.